MONITORING ACOUSTIC EMISSIONS AND ELECTRICAL SIGNALS DURING THREE-POINT BENDING TESTS PERFORMED ON CEMENT MORTAR SPECIMENS

C. STERGIOPOULOS[*†], I. STAVRAKAS[*], G. HLOUPIS[*], A. KYRIAZOPOULOS[*], D. TRIANTIS[*], C. ANASTASIADIS[*] AND J. STONHAM[†]

[*] Dept. of Electronics, Technological Educational Institute of Athens
Ag. Spyridonos, 12210, Egaleo, Athens, Greece
e-mail: csterg@ee.teiath.gr, research.ee.teiath.gr

[†] School of Engineering & Design, Brunel University
Kingston Lane, Uxbridge, Middlesex UB8 3PH, UK
e-mail: john.stonham@brunel.ac.uk, www.brunel.ac.uk

Key words: Acoustic Emissions, Pressure Stimulated Currents, b-Value Analysis, Cement Mortar

Abstract: Three-point bending tests were performed on cement mortar beams of rectangular cross section. The specimens were subjected to abrupt compressive step loading while simultaneous Acoustic and Electrical Signal Emissions were recorded. In order to evaluate the development of the fracture process, characteristics of acoustic emissions and electrical current signals were studied and compared by isolating specific time frames that correspond to every step up to the fracture. In terms of time series cumulative energy of Pressure Stimulated Currents (PSC) and Acoustic Emissions (AE) were compared. Moreover, cumulative frequency distribution (Gutenberg–Richter relationship) and b-value analysis was performed in the AE using Gutenberg–Richter and Aki's methods. The objective of the experiments was to study the variation of AE based b-value with respect to time. It was observed that the AE based b-value analysis serves as a tool to identify the development of cracks and assess damage evolution.

1 INTRODUCTION

Cement-based materials are widely used in constructions. Mechanical testing of such materials is of vital importance in order to evaluate their use on various applications. In situ and laboratory, health monitoring of cement-based material constructions and testing techniques have been adopted by scientists and engineers. Under this concept several non-destructive tests (NDT) have been developed for real-time mechanical status monitoring and damage assessment [1].

It is known that when a brittle material is subjected to mechanical loading a weak electrical current is generated and propagates in the bulk of the materials due to charge separation processes and local polarizations. The experimental protocol that is adopted in order to detect and record the electrical currents is known as Pressure Stimulated Currents (PSC) technique [2]. The PSC technique has been applied on materials like natural stones (i.e. marble [3-5] and amphibolites [6]) and cement-based materials [7-8]. Previously conducted experiments using the PSC technique on cement-based materials involved both axial compressional tests and Three-Point Bending (3PB) tests. The specimens were subjected to various modes of mechanical loading like constantly increasing

load up to fracture, and stepwise load increase.

Previous works on marble, amphibolites and cement based materials have shown that the qualitative and quantitative characteristics of the PSC recordings provide clear information regarding the level of mechanical damages of the material and the remaining strength until the fracture [7-11].

Another commonly used technique for non-destructive evaluation of materials is the detection of transient elastic waves generated from the stress concentration in the bulk of a specimen when it is subjected to mechanical loading and causes the generation and propagation of cracks [12]. These elastic waves are known as Acoustic Emissions (AE). This technique has been adopted from several researches in order to monitor the crack generation and propagation processes [13-17]. Regarding the cement based materials the AE technique has been used to monitor the microfracture processes taking place in the bulk of a specimen [12]. Laboratory experiments conducted when cement-based specimens were subjected to externally applied mechanical loading have provided significant information regarding the characteristics of the AE recordings during all regions of the mechanical behavior of the specimen [18-19].

Recently, an attempt was made for studying the results and effectiveness of the AE monitoring technique on brittle materials when compared with similar techniques adopted in seismology [17, 20]. Specifically, the Gutenberg–Richter relation that monitors the distribution of the cumulative frequency of occurrence versus magnitude has been evaluated in the past. This relation shows that the log-linear slope of the extracted curves provides significant information regarding the damage development in the bulk of a specimen. Another approach besides the Gutenberg–Richter relation is the Aki's method that uses the discrete frequency distribution of the recorded magnitudes. Both methods are considered as valid and applicable.

In this work concurrent recordings of PSC and AE were conducted while a cement mortar beam was subjected to 3PB mechanical loading. The mechanical load was continuously increasing in a step-like form from an early load level up to the fracture of the specimen. The characteristics of the PSC and AE are studied in order to investigate similarities and pre-failure characteristics of the recorded signals. Specifically, the temporal variations of the amplitudes and the energy are presented and discussed with respect to the applied load level. Finally, an attempt was made for correlating the results of the the b-value analysis following the GBR and Aki's approach to the applied mechanical load.

2 EXPERIMENTAL TECHNIQUE AND ANALYSIS

2.1 Experimental technique

The cement mortar beams were subjected to 3PB tests. Specifically, the mechanical load was applied in a step-like form. A gradual increase of the load from a low level until the fracture was performed by applying sequentially abrupt and high rate loadings. Each loading step was conducted from an initial level L_{n-1} up to a higher one L_n as shown in Figure 1a where n is the number of each consequent step.

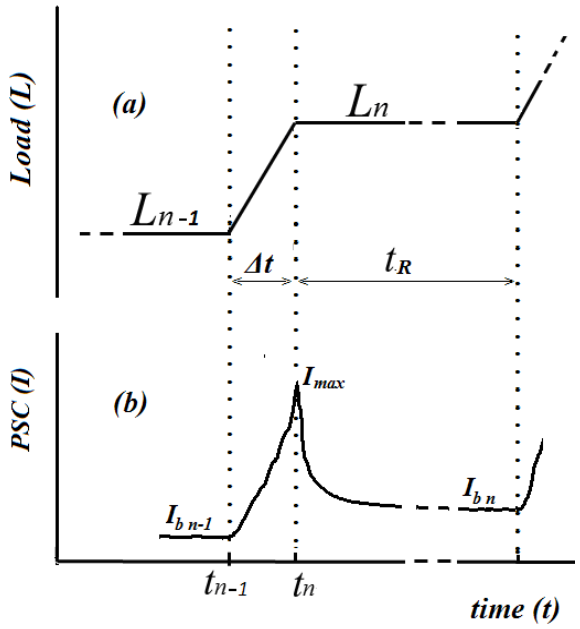

Figure 1: (a) A typical loading step applied during the 3PB test and (b) the corresponding PSC.

The mathematical formulation that describes the mechanical loading is given by the following equation:

$$L(t)=\begin{cases} L_{n-1}=constant & t<t_{n-1} \\ L_{n-1}+r(t-t_{n-1}) & t_{n-1}<t<t_n \\ L_n=constant & t_{n-1}<t<t_n+t_R \end{cases} \quad (1)$$

where L_{n-1} and L_n is the low and high level of the n[th] step correspondingly. Taking under consideration the dimension and the geometry of the specimens used during the experiments, the loading rate, r (see Equation 1) and $\Delta L = L_n - L_{n-1}$ were selected to vary from 0.2kN/s up to 0.4kN/s and 1kN up to 1.5kN respectively, in accordance to the protocol of the technique. The duration t_R that the load was kept constant at the high level L_n was selected to be $t_R = 100s$ approximately. In this work the PSC and the corresponding AE were studied during the period of t_R for each step. The aim was to detect the variations of specific characteristics and parameters of the PSC and AE during the time frame t_R of each step.

2.2 PSC analysis

Published works have shown that when a brittle material is subjected to 3PB tests the recorded PSC shows a deterministic behaviour [7, 20]. Specifically, when applying 3PB tests following a step like increase of the mechanical load, the recorded PSC (I) increases during the short time Δ_t reaching a peak value of $I_{\max}$ at the time that the load reaches the value of L_n as shown in Figure 1b. Consequently, the PSC starts relaxing until reaching a background level $I_{b\,n}$ during a time shorter than t_R. The value of $t_R = 100s$ was selected in order to provide enough time to the PSC for relaxing and reaching $I_{b\ n}$ level. During the time frame t_R the PSC cumulative energy is calculated by the following equation:

$$E_n^{PSC} = \int_{t_n}^{t_n+t_R} I \cdot dt \quad (2)$$

where E_n^{PSC} is the cumulative energy during the n[th] step.

2.2 AE analysis

In relation to the PSC cumulative energy E_n^{PSC} the corresponding AE cumulative energy E_n^{AE} is calculated by the following equation:

$$E_n^{AE} = \sum_{t_n}^{t_n+t_R} e_i(t_i) \quad (3)$$

where $e_i(t_i)$ is the AE recorded energy at time t_i within t_R of each step. During each loading step the total number N of the AE events is also measured.

Additionally, the amplitude distribution of the AE events can be analyzed using the "b-value analysis". The b-value is defined as the log-linear slope of the frequency – magnitude distribution of the AE events. In case of AE technique, the Gutenberg–Richter (GBR) modified relationship is given by the following equation [17, 21]:

$$log_{10}N(M) = a - b(\frac{A_{dB}}{20}) \quad (3)$$

where A_{dB} is the peak amplitude of the AE events in decibels, N is the number of AE hits having amplitude greater than a predefined threshold, a is an empirical constant and b is the b-value.

A second approach to estimation of the b-value is the Aki's method [17]. According to this method the b-value is calculated by the following equation:

$$b = \frac{20 \cdot log_{10}e}{< A_{dB} > - A_c} = \frac{8.686}{< A_{dB} > - A_c} \quad (4)$$

where $< A_{dB} >$ is the mean amplitude and A_c is the amplitude threshold that was set at 40dB.

2.3 Experimental set-up

The basic experimental setup for measuring PSC and AE is shown in Figure 2. Two rigid metallic cylindrical rods supported the cement mortar beam. The distance of each rod's centre from the centre of the beam was 85mm.

Another identical rod was placed on the upper side of the beam, on its centre, where the load would be applied during the 3PB process. All three points were electrically isolated using Teflon plates with 2mm thickness.

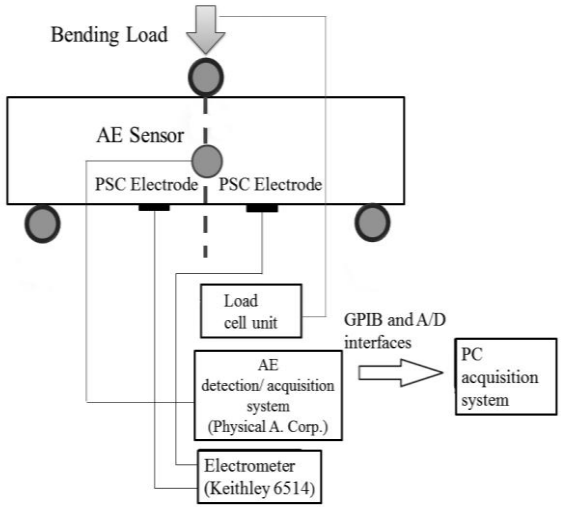

Figure 2: The experimental setup to measure PSC and AE concurrently during 3PB tests.

In order to capture the PSC a high sensitivity electrometer was used (Keithley, Model 6514). For further processing, data were recorded and stored in a computer in real time through a GPIB interface. A pair of electrodes was used for sensing the PSC. The electrodes were attached to the surface of the beam at the tensile zone of the beam. The distance of each electrode's centre from the centre of the beam was 20mm. Their shape was orthogonal with dimension 30mmx10mm. The electrodes were made of a thin foil of copper. Before their attachment on the surface of the specimen, a silver conductive layer was on the area under the electrode.

The system that was used to detect and record the AE is the PCI-2 AE acquisition system (Physical Acoustics Corp). The acoustic sensor was attached to the front end of the beam right at its centre. This location was selected for better focusing on the AE events that will be generated due to the cracking process developed at this particular region. In order to improve the acoustic coupling of the sensor its effective area was covered with a layer of silicon grease before attached to the surface of the cement mortar beam. For recording and processing AE data the Physical Acoustics Corp. Noesis software was used. The threshold for detecting acoustic events was set at 40dB. Moreover, a frequency cut-off filter was installed at the input of the acoustic sensors. The filter was used for discarding AE events having frequencies lower than 20kHz. This way, any AE events coming from external sources would be ignored.

A data acquisition device (Keithley, model KUSB-3108) was used for recording the applied mechanical load. The experimental setup was installed in a Faraday shield to avoid any external electrical noise from affecting the measurements.

3 MATERIALS

The experiments were conducted on cement mortar specimens. Ordinary Portland Cement (OPC) was used as the basic ingredient of the mixture. The OPC was mixed with sand, consisted of fine aggregates, and water at a weight ratio 1:3:0.5 respectively. A refinement process was performed on the aggregates in order to collect the ones that their size was from 0.6mm up to 3.0 mm approximately. Low speed was maintained during the mixing process for achieving the best moisturizing of the cement. The mixture was poured in wooden moulds and remained there for 24 hours. An estimation of the produced beams showed that their porosity is 8% approximately. The dimensions of the beams were 200mm long with a square cross-section of 50mmx50mm. After been extracted of their moulds, the specimens were stored in a special chamber for 90 days in order to obtain 95% of their total strength [22]. During the period of their storage the conditions remained constant (22°C and 75%–80% humidity). After conducting preliminary 3PB strength tests the fracture limit of the produced specimens was 4.8±0.3kN.

4 EXPERIMENTAL RESULTS

During the experiments four loading steps were conducted while an attempt was made to conduct a fifth one during which, the specimen

failed. Figure 3a shows the temporal behaviour of the mechanical load. In the beginning of the tests the specimens were pre-loaded L_0 at 0.2 kN. The value of the fracture load of the beam in the presented experiment was L_f =5.6 kN. In Table 1 the values of load for each step are shown.

Table 1: Values of mechanical load and the loading rate for each step

n-step	L_{n-1} (kN)	L_n (kN)	L_n/L_f *	r (kN/s)
1	0.21	1.54	0.28	0.30
2	1.53	2.73	0.49	0.23
3	2.72	3.94	0.71	0.29
4	3.95	5.00	0.90	0.25

*L_f : The fracture load equals to 5.6kN

At the same time the PSC was detected at the centre of the tensile zone of the specimen and its temporal variation is shown in Figure 3b. As expected, the recorded PSC is characterized by spikes. Specifically, during the load increase, the PSC exhibits a maximum value $I_{\max}$ and consequently the PSC relaxes when the load is kept constant. These results agree with previous works [7]. The recorded PSC is attributed to the creation, development and spread of micro cracks which generate charge separation phenomena. Systematic measurements have shown the following: The value of $I_{\max}$ depends on both the loading rate r, the applied mechanical load L_n and the value of $I_{b\,n}$ where the PSC relaxes after completing the load step L_{n-1}. The values of $I_{\max}$ and $I_{b\,n}$ are presented in Table 2. In the same table the value of $I_{\max}/r$ for each step has also been presented. This value exhibits an increasing tendency together with L_n. The above observation needs further study.

Figures 3c and 3d show in time correspondence the recorded amplitude and energy of the AE events during the experimental procedure. It is clear that during the moment the PSC reaches $I_{\max}$, AE events of high amplitude and energy are recorded.

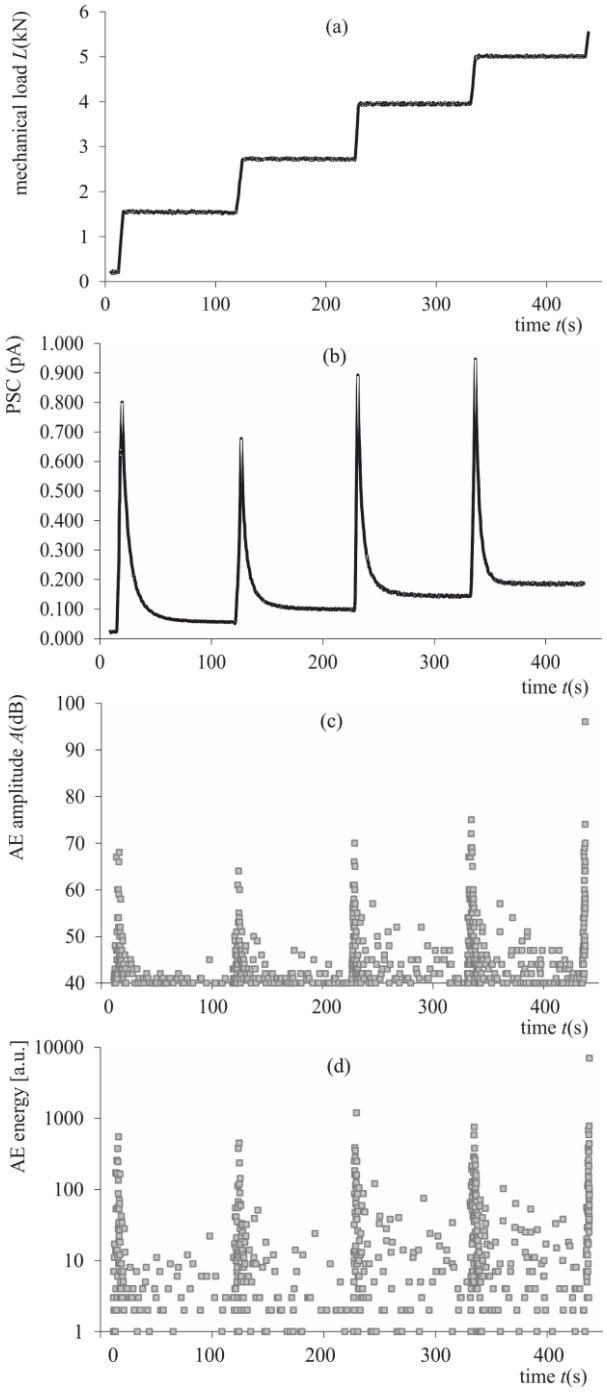

Figure 3: (a) mechanical load, (b) PSC recordings, (c) Amplitude of AE events, (d) Energy of AE events.

Table 2: PSC related quantities for each step

n-step	L_n/L_f	$I_{\max}$ (pA)	$I_{b,n}$ (pA)	$I_{\max}/r$ (fC/N)	E_n^{PSC} $(pA^2 \cdot s)$
1	0.28	0.72	0.05	2.39	2.10
2	0.49	0.63	0.09	2.69	2.25
3	0.71	0.81	0.13	2.81	4.17
4	0.90	0.85	0.15	3.42	4.94

Table 3: The number of AE events and the corresponding cumulative energy for each step

n-step	L_n/L_f	Number (N_n) of AE events	E_n^{AE} [a.u.]
1	0.28	78	907
2	0.49	95	1075
3	0.71	98	2098
4	0.90	145	3450

Figure 4 shows the cumulative energy E_n^{PSC} and E_n^{AE} of PSC and AE respectively in relation to the normalized load L_n/L_f. The values of E_n^{PSC} and E_n^{AE} are shown in Table 2 and Table 3 respectively.

The cumulative energies exhibit similar behaviours as shown in Figure 4. Specifically, during the two first steps where the applied load is below $0.5L_f$ the cumulative energies are practically constant. On the contrary, when the applied mechanical load becomes higher than $0.5L_f$ the corresponding energy values are significantly increased implying the increased concentration of damages in the bulk of the specimen.

For each one of the four steps within t_R the values N_n of the AE events were calculated (see Table 3). Although no significant increase of N relative to the previous step is observed during step 3, the recorded events correspond to higher values of energy.

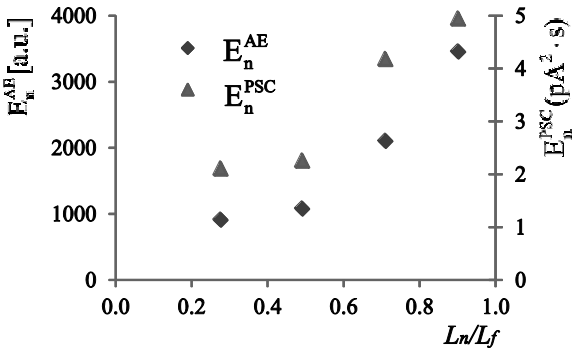

Figure 4: AE and PSC cumulative energies with respect to the normalized load L_n/L_f of the four loading steps.

The recorded values of AE amplitudes were processed using in order to carry out a b-value analysis. A step of 1dB was selected beginning from the threshold value of 40dB until the maximum recorded value. For each group of AE that corresponds to each of the four steps the log cumulative frequency log(N) graph was plotted for the time frame t_R. As shown in Figure 5.

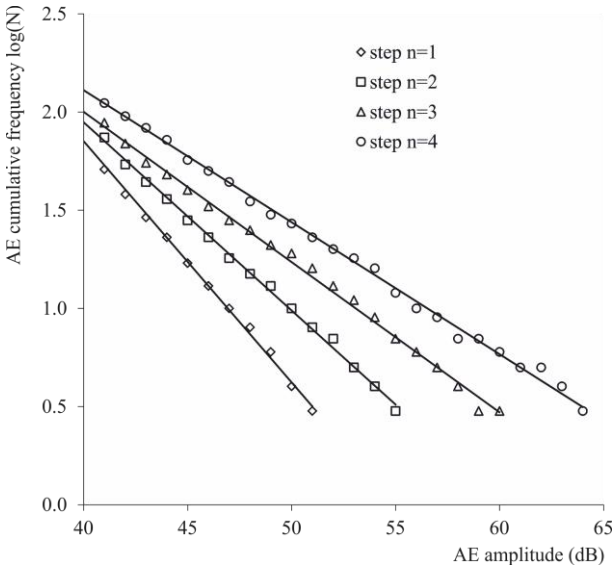

Figure 5: the distribution of the AE cumulative frequency (log(N)) with respect to the amplitude of the AE events.

The corresponding linear trend was calculated using the least-squares method of fitting curves, based on Equation 3 for data points when the log(N) >0.5. The fitting results of the b-value and the corresponding error spaces are presented in Table 4.

Table 4: b-values from GBR and Aki's method

n-step	L_n/L_f*	b-value	
		GBR method	Aki's method
1	0.28	2.46 ±0.28	3.12±0.36
2	0.49	1.97±0.23	2.81±0.29
3	0.71	1.53±0.16	1.72±0.18
4	0.90	1.35±0.11	1.54±0.13

The b-values were also calculated applying the Aki's model approach, substituting the value of $< A_{dB} >$ in the formula given by Equation 3. In both cases it is observed that the b-value

becomes lower as the applied mechanical load (L_n) decreases. Aki's model provides in general higher b-values.

Figure 6 shows the behavior of the b-values with respect to the corresponding mechanical load level for both the GBR and Aki's approach. The observation that when the applied load reaches the vicinity of fracture the b-value becomes lower is expected since the high stress concentrations in the bulk of the specimens cause more AE events of high amplitudes and energy. Taking into consideration that low amplitude AE events are mainly attributed to the new crack formations and high amplitude and energy AE events are attributed mainly to the crack extension and propagation processes it is expected that when reaching fracture the two physical processes to co-exist and provide lower slope to the GBR curve.

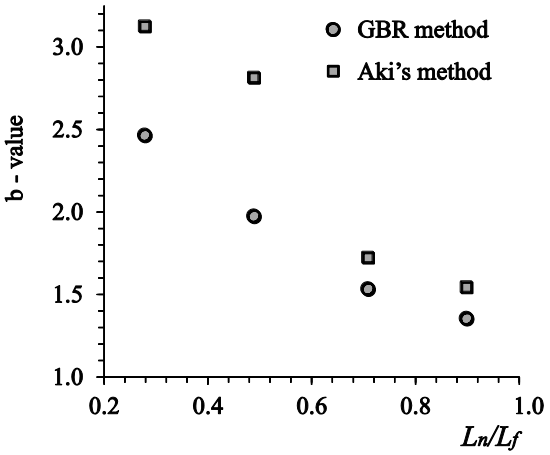

Figure 6: Calculation of b-value using both GBR and Aki's approach.

5 CONCLUSIONS

A combined experimental research of PSC and AE is introduced in this work. PSC and AE techniques have been applied on cement mortar beams subjected to three-point bending tests. The bending load was applied progressively with abrupt increments so that the beam remains under a constant bending load for a significant time.

The experimental results exhibit the following:

When the constant bending load exceeds 60%, then, the cumulative AE and PSC energies increase significantly. The PSC peaks are correlated with increased amplitudes and energies of the acoustic events.

Using the b-value analysis it was shown that the b-parameter can give a clear piece of information related to the difference in magnitude between the applied constant bending load and the fracture load of the cement mortar beams. In other words, the more the bending load approaches the fracture load, the b-value decreases progressively to values smaller than 1.5.

It is mandatory that systematic experiments be carried out for the verification of the b-value dependence on the value of the bending load.

If such an empirically observed dependence is verified, then, the b-value analysis technique might be applied to constant bending load experiments, following an abrupt increase of the load. This could be an acceptable non-destructive method of fracture load estimation.

Finally, it is worth studying explicitly the characteristic PSC relaxation parameters in bending experiments using the fore-mentioned application of bending load as it has already been used in uniaxial compressive stress experiments on cement mortar beams [11].

ACKNWOLEDGMENTS

This research has been co-funded by the European Union (European Social Fund) and Greek national resources under the framework of the "Archimedes III: Funding of Research Groups in TEI of Athens" project of the "Education & Lifelong Learning" Operational Programme.

REFERENCES

[1] Kumar Mehta, P. and Monteiro, P.J.M., 2005. *Concrete: Microstructure, Properties, and Materials*. McGraw-Hill Prof Med/Tech.

[2] Stavrakas, I., Triantis, D., Agioutantis, Z., Maurigiannakis, S., Saltas, V., Vallianatos, F. and Clarke, M., 2004 Pressure stimulated currents in rocks and

their correlation with mechanical properties. *Nat. Haz. Earth Sys*. **4 (4)**: 563 -7.

[3] Anastasiadis, C., Triantis, D., Stavrakas, I. and Vallianatos, F., 2004 Pressure stimulated currents (PSC) in marble samples after the application of various stress modes before fracture. *Ann. Geophys.* **47**:21–8.

[4] Triantis, D., Stavrakas, I., Anastasiadis, C., Kyriazopoulos, A. and Vallianatos, F., 2006 An analysis of pressure stimulated currents (PSC), in marble samples under mechanical stress. *Phys. Chem. Earth* **31**:234–9.

[5] Anastasiadis, C., Triantis, D., Hogarth, CA., 2007 Comments on the phenomena underlying pressure stimulated currents (PSC) in dielectric rock materials. *J. Mater. Sci.* **42**:2538–42.

[6] Triantis, D., Anastasiadis, C., Vallianatos, F., Kyriazis, P. and Nover G., 2007 Electric signal emissions during repeated abrupt uniaxial compressional stress steps in amphibolite from KTB drilling. *Nat. Haz. Earth Syst. Sci.* **7**:149–54.

[7] Kyriazopoulos, A., Anastasiadis, C., Triantis, D. and Brown, J.C., 2011 Non-destructive evaluation of cement-based materials from pressure-stimulated electrical emission - Preliminary results. *Constr. Build. Mater*. **25**: 1980–90.

[8] Triantis, D., Stavrakas, I., Kyriazopoulos, A., Hloupis, G. and Agioutantis, Z., 2012 Pressure Stimulated Electrical Emissions from cement mortar used as failure predictors. *Int. J. Fracture* **175:** 53-61.

[9] Anastasiadis, C., Stavrakas, I., Triantis, D. and Vallianatos, F., 2007 Correlation of pressure stimulated currents in rocks with the damage variable. *Ann. Geophys.* **50**:1–6.

[10] Triantis, D., Stavrakas, I., Anastasiadis, C., 2008 The Correlation of Electrical Charge with Strain on Stressed Rock Samples. *Nat. Hazard Earth Sys.* **8**:1243–8.

[11] Alexandridis, A., Triantis, D., Stavrakas, I. and Stergiopoulos, C., 2012 A neural network approach for compressive strength prediction in cement-based materials through the study of pressure stimulated electrical signals. *Constr. Build. Mater*. **30**:294–300.

[12] Grosse, C.U., Ohtsu, M., 2008. *Acoustic Emission Testing. Basic for Research Applications in Civil Engineering*. Springer – Verlag.

[13] Lavrov, A., 2005 Fracture-induced Physical Phenomena and memory Effects in Rocks: A Review **41**:135-49.

[14] Yamada, I., Masuda, K. and Mizutani, H., 1989 Electromagnetic and acoustic emission associated with rock fracture. *Phys. Earth Planet Inter*. **57**:157-68.

[15] Tatum, P.J., 2003 The measurement of acoustic emissions to detect embrittled brazed joints, **39**:79–82.

[16] Lockner, D., 1993 The role of acoustic emission in the study of rock fracture. *Int. J. Rock Mech. Min. Sci. Geomech. Abstr*. **30**:883–99.

[17] Vidya Sagar, R., Raghu Prasad, B.K. and Shantha Kumar S., 2012 An experimental study on cracking evolution in concrete and cement mortar by the b-value analysis of acoustic emission technique, *Cement Concrete Res.* **42**:1094-104.

[18] Landis, E.N. and Shah S.P., 1995 The influence of microcracking on the mechanical behavior of cement based materials. *Adv. Cem. Based Mater*. **2**:105-18.

[19] Landis, E.N., 1999 Micro–macro fracture relationships and acoustic emissions in concrete. *Constr. Build. Mater.* **13**:65-72.

[20] Kyriazis, P., Anastasiadis, C., Stavrakas, I., Triantis, D. and Stonham, J., 2009 Modelling of electric signals stimulated by bending of rock beams. *Int. J. Microstruct. Mater. Prop.* **4**: 5-18.

[21] Colombo, I.S., Main, I.G. and Forde, M.C., 2003 Assessing damage of reinforced concrete beam using b-value analysis of Acoustic emission signals. *J. Mater. Civ. Eng.* **ASCE:**280–6.

[22] Kosmatka, S., Kerkhoff, B. and Panarese W., 2003 *Design and Control of Concrete Mixtures, 14th ed.* Portland Cement Association.